Turk J Elec Eng & Comp Sci, Vol.18, No.3, 2010, © TÜBİTAK
doi:10.3906/elk-0912-14

Modeling and simulation strategies in high frequency surface wave radars

Levent SEVGİ
Department of Electronics and Communication Engineering, Faculty of Engineering
Doğuş University, Zeamet Sok. No.21, Acıbadem, 34722 Kadıkoy, İstanbul-TURKEY
lsevgi@dogus.edu.tr

Abstract

Surface Wave High Frequency Radars (SWHFR) are taken into account in the content of modeling and simulation challenges. Examples related to multi-mixed path surface wave propagation, radar cross section (RCS) prediction, and total radar echo showing target, clutter, noise, and interference are presented.

1. Introduction

Safe maritime transportation necessitate precise maritime traffic supervision and control. This is especially required in densely operated port approaches, straits and narrow waterways. The mission starts with effective surveillance therefore integrated maritime surveillance (IMS) systems are of great interest [1-5]. Sensors include (but not limited to) radars from high frequencies to microwaves and millimeter waves, optical sensors, daylight and thermal (infrared) cameras, acoustic, ultrasonic, chemical and biological sensors, etc. IMS systems have been widely used for both military and commercial maritime traffic supervision and control. In addition to surveillance, communication, control, command and fire-control may also be required in some of these IMS systems. A typical IMS scenario is pictured in Figure 1. Although Turkey is shown in the figure, it may be any other country, such as Greece, Italy, Egypt, England, Germany, France, China, Australia, Sri Lanka, etc.

The sensors within the IMS system in Figure 1 are surface wave high frequency radars (SWHFR). Depending on the mission of the IMS system there may be a few other sensor alternatives; but all should have detection, tracking, profiling, classification, imaging capabilities in order to increase system performance. Traditional land-based microwave (MW) radars may be used but these are limited to operate within line-of-sight (LOS). Even by elevating the radar platforms the maximum range is limited to 50-60 km. The area can be covered by a number of airborne MW radars, but these provide only a snap shot in time of activity within the area and operational costs are very high. Sky wave high frequency (HF) radars can be used for this purpose, but they need large installations, are expensive and detection of surface targets is still limited. An optimum and reliable sensor seems to be the SWHFR.

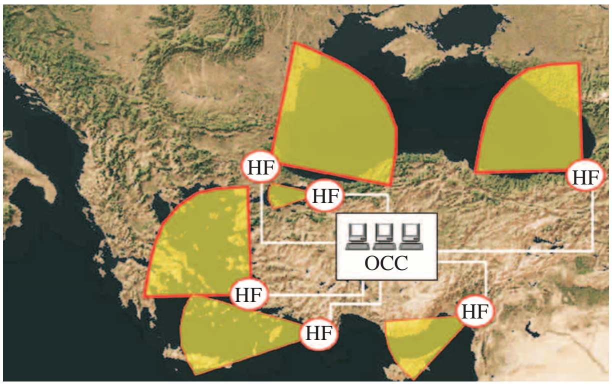

Figure 1. A typical HFSWR based IMS system.

This paper reviews modeling and simulation studies related to the HFSWR. In Section 2, HFSWR and its role within IMS is discussed. Some HFSWR related challenging problems that still need to be addressed are given in Section 3. Modeling and simulation examples are presented in Section 4. Finally, the conclusions are listed in Section 5.

2. Surface wave HF radars

HFSWR for long-range surveillance is a developing technology [1-4] which has already demonstrated excellent capabilities in the long-range detection of ships and aircraft as well as icebergs, and in the remote sensing of the ocean environment. Operation at the lower end of the HF band allows the radar to achieve ranges up to 400-500 km by means of surface waves, where the high conductivity of seawater results in relatively low attenuation of the vertically polarized radio waves.

A typical HFSWR scenario is pictured in Figure 2. The surveillance area is illuminated on transmit using a broad beam up to 120° in azimuth. Echoes from all objects within the coverage area are received by a linear array of antennas. Beam Synthesis is used to generate simultaneous narrow receive beams. Coherent integration (CI) and other signal processing techniques are used to isolate the target signal from the noise and clutter. Return echoes are sorted according to range, velocity (Doppler), and bearing. Detections are compared against a detection threshold chosen to maintain a Constant False Alarm Rate (CFAR). Those detections exceeding the threshold are declared as detections. A Tracking algorithm associates successive detections to form tracks.

HFSWR is capable of supplying range, bearing and velocity but not altitude information. Range resolution is proportional to the bandwidth of transmitted waveforms. For example, for a 20 kHz waveform, resolution is about 7.5 km. Azimuth resolution is proportional to the aperture of the receive array, and a 24-element array with 1/2 wavelength spacing corresponds to a beam width of approximately 5 degrees. This translates to a cross range of 30 km at 400 km range. Finally, velocity resolution is proportional to the CI time, and typically, are 2 m/s and 0.2 m/s for air and surface targets, respectively. Targets are resolved if separated in at least one dimension. Although these seem to be moderate, accuracies better than one tenth of the basic resolution can be achieved.

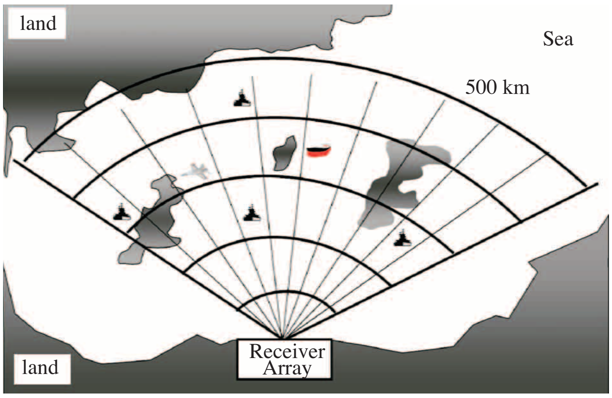

Figure 2. A typical HFSWR scenario: Range, cross-range resolution and radar cells [4].

HFSWR operates in densely occupied 2-10 MHz frequency region and heavily relies on signal processing techniques, so system operation requires HF spectrum monitoring to optimize performance by continually moving to unoccupied channels. Also, frequency hopping is a must to support interference suppression. Adaptive algorithms and coded waveforms must be used in suppressing external interference and ionosphere-reflected multipath signals. The status of the ionosphere should be monitored in order to select a radar frequency that minimizes ionospheric returns over range of interest.

3. Problems and challenges related to HFSWR

HFSWR signal environment is extremely complex. Noise power which limits the detection level fluctuates as a function of time of day and season and is constant for all ranges [2, 24]. External Noise increases by 15 - 20 dB at night. Wind dependent sea clutter is dominated by Bragg scatter [26-29] that results in two dominant peaks. Second and higher order scattering from sea waves results in other lesser peaks and a continuum. The continuum dominates the external noise during daylight hours, out to about 200 km. Ionospheric conditions change with time of day and season, and generally produce a strong reflection at ranges corresponding to the E and F layers (100 and 200 km). Interference from other users of the HF band, such as long range skywave communication, gets worse at nights.

Problems and challenges related to SWHFR may be listed as follows.

Wave propagation :

One challenge, as shown in Figure 2, is to find out the optimum location and coverage for HFSWRs. This necessitates accurate path loss calculations and/or measurements. Estimation of typical path losses between the radar transmitter and the target at various operating frequencies requires a good propagation model. The model environment is a spherical Earth with imperfect, rough surface, and variable refractivity above [5-15]. One difficulty in determining the path loss for HFSWR is the existence of multi mixed-paths between the radar and surface targets [6-8]. Early analytical models [5, 6] are valid for homogeneous propagation path over smooth spherical Earth with impedance boundary conditions. Propagation effects over multi-mixed smooth paths (e.g., sea-land transitions) can be predicted via Millington approach [7]. ITU has also published curves and techniques for HF path loss calculations [5].

Parabolic equation (PE) method has been extensively used in multi-mixed path propagation modeling [12-

14]. Finite-element, finite-difference, and split step Fourier Transform based PE models have been successfully used in HFSWR path loss predictions [14,15]. A mixed-path propagation prediction example is plotted in Figure 3. The scenario includes a 3-segment 40 km mixed path with a 10 km long, 250 m high Gauss-shaped island at a distance of 15k m. Electrical parameters for the sea and island are $\sigma = 0.002\ S/m$, $\varepsilon_r = 10$, and $\sigma = 5\ S/m$, $\varepsilon_r = 80$, respectively. On top, signal strength vs. range/height is given. At the bottom, path loss vs. Range along this three-section path is shown. Observe the sharp increase in the attenuation at the sea-land discontinuity, signal recovery in the front slope of the island, the additional signal attenuation at the back slope of the island, and finally the signal recovery at the land-sea discontinuity.

Antenna design:

Planar monopole arrays over lossy ground are used as both transmit and receive antenna elements for HFSWR systems. The antennas are mostly located above a ground screen to reduce ground and coupling losses. Therefore, good ground screen design is very important. On the other hand, both transmit and receive arrays should have deep overhead nulls to prevent ionospheric coupling of undesired signals. Meeting all these requirements may only be possible via a good design of arrays and studies are still required to better design new types of antenna arrays [20-22]. HFSWR uses signal processing techniques to eliminate noise, clutter and interference, and signal processing gains of 40 to 60 dB may be reached. Most of this gain is lost at the beginning if transmit and receive antenna arrays are not designed properly.

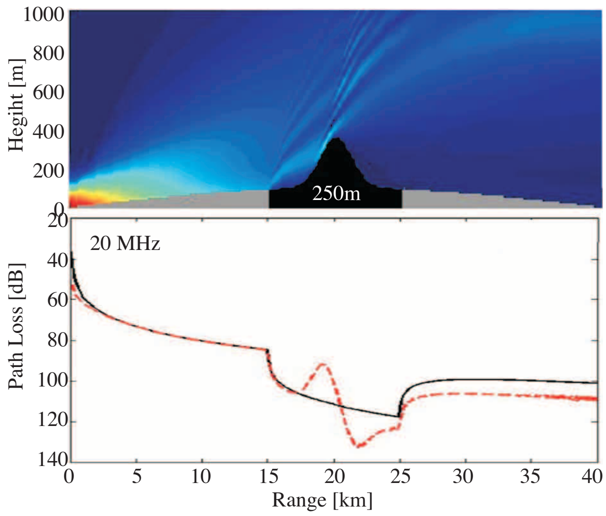

Figure 3. A typical mixed-path propagation scenario and longitudinal signal variation.

Target reflectivity analysis:

Radar wavelengths of HFSWRs are on the order of 10-100 m. Therefore radar targets' sizes and radar signal wavelengths are in the same order. The RCS regime of interest is the resonance regime. In this RCS region the target contributes to its RCS as a whole, and high frequency asymptotic techniques, such as geometric optics (GO), physical optics (PO), physical theory of diffraction (PTD), etc., are not applicable. Fortunately, there are powerful time- and frequency-domain simulation methods, with which good estimate of RCS can be achieved [22, 32, 33]. An effective RCS prediction tool is introduced in [33] which can be used as an education tool as well as a research package. The tool discretizes a given target and creates both finite-difference time-domain

(FDTD) and method of moments (MoM) discrete models. It then simulates RCS behaviors of this target with both FDTD and MoM codes and verifies one against the other.

Two example outputs of this tool are given in Figures 4 and 5. Figure 4 belongs to video recording (i.e., frame capturing) of a discrete target during the FDTD simulations. Here, a 50 m long Tarantual III frigate and scattered near fields at four different time instants are given. The frigate is also pictured there. Figure 5 compares RCS vs. frequency of single and double flying F-16 targets. As shown in the figure, as the frequency changes the RCS interactions between nearby targets changes drastically.

Total radar echo:

The HFSWR radar echo contains signatures of target RCS, noise, clutter, and interference. These are all radar waveform-dependent and vary with frequency as well as with the type of radar. The detection performance of HFSWR is limited by external noise [24, 25]. External noise may be atmospheric, galactic or man-made. For frequencies below 10 MHz, atmospheric noise usually dominates. At the lower end of the HF band the external noise level is approximately 40-60 dB higher than thermal noise and is subject to diurnal and seasonal variation. A good design of a HFSWR system requires a long term environmental noise monitoring and statistical evaluation [25]. Ionopshere is also a severe interference source/media in HFSWR systems. Ionospheric signal may be viewed as multipath clutter or self-interference. Ionospheric self-interference may be divided into two main categories, specifically, *near vertical incidence (NVI) clutter* and *range folded clutter.* With NVI clutter, the HFSWR signal travels vertically from the radar and is reflected from an ionospheric layer directly back to the radar. Range folded clutter occurs when the signal is directed at an angle other than vertical. Understanding and eliminating ionospheric interference is still a challenge in HFSWR systems.

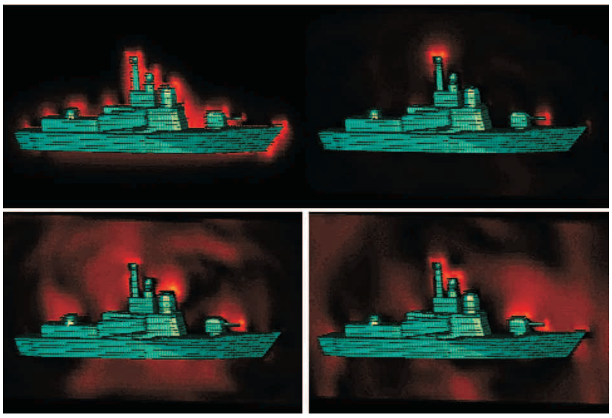

Figure 4. EM wave - Tarantual III frigate interaction.

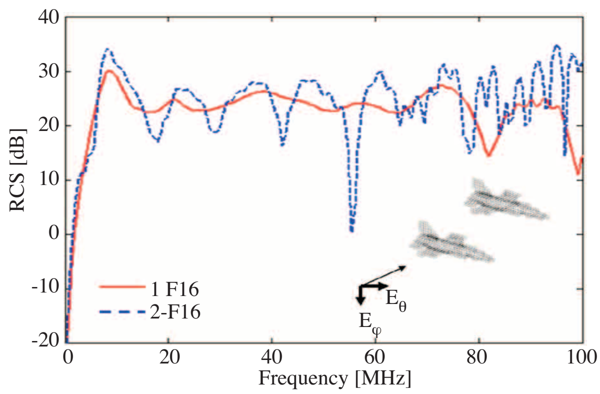

Figure 5. Two F-16 flying side-by-side and their RCS vs. frequency curves.

Sea clutter is also unwanted, self-generated interference for HFSWR systems. The clutter can be characterized as a distributed non-directional source. Sea clutter is the result of the interaction of the radiated electromagnetic wave with ocean waves. The dominant contribution is produced by scatter from ocean waves having a wavelength half that of the radar wavelength and moving radially to and away, from the radar site. This first order resonant scatter result in two dominant peaks called Bragg lines. The two dominant peaks (Bragg lines) [26-30] at two distinct Doppler frequencies $f_b = \pm\sqrt{g/\pi\lambda} \approx 0.102\sqrt{f_{MHz}}$ in Hz corresponding to the velocities of the propagation of these ocean waves [10]. Here, λ is the radar wavelength, f is the radar frequency in MHz, and g is the acceleration due to gravity. Sea waves are trochoidal and Bragg resonant scatter will also occur at harmonics of the principal wavelength. These results in second order peaks in the spectrum.

HFSWR systems use constant false alarm rate (CFAR) detector in the frequency (Doppler) domain, therefore intelligent CFAR algorithms are required. Testing these algorithms necessitates data either recorded or synthetically generated. Synthetic data generation for these tests is another challenge. It requires numerical modeling of environmental noise, ionospheric reflections, interfering sources, and the target [26-31]. All fluctuate randomly with the time so the signal environment is *stochastic*. Usually, the target signal is embedded within a background (noise + clutter) signal and/or obscured by interference; i.e., its power level is much less than the others. The process of extracting target information from the total echo is called (stochastic) signal processing and performed via powerful, intelligent algorithms. The power of these algorithms comes from the physical and statistical understanding of the target, noise, clutter and interfering signals, and computer generation of the synthetic signal environment.

Total HFSWR echoes generated synthetically are shown in Figure 6 [34]. Here, SNR=13 dB but CNR=30 dB, which means the target is embedded in the clutter signal. The figure represents one HFSWR cell in the frequency-domain where targets are distinguished using their radial velocities with respect to the radar (note that horizontal scale is normalized to the Brag Frequency).

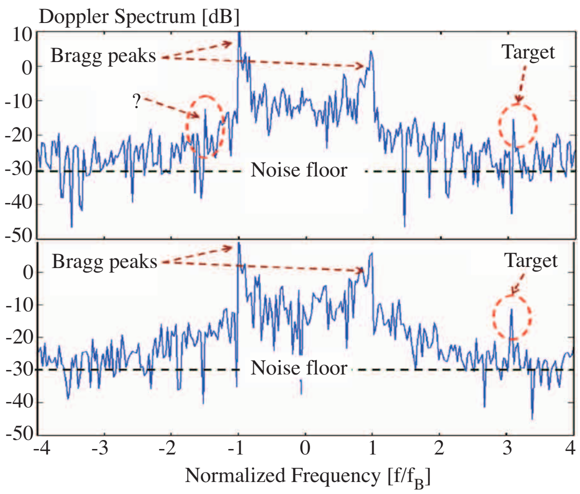

Figure 6. Two Doppler spectra showing total HFSWR echoes. The spectra contain noise, clutter and target (SNR=13 dB, CNR=30 dB, Noise floor is set to -30 dB).

The Bragg peaks ($f_b \approx \pm 0.102\sqrt{f_{MHz}}$) around $\pm 0.25\,Hz$ (which are normalized to $\pm 1\,Hz$) correspond to the radar carrier frequency of 6 MHz. Assume this carrier frequency is removed at the front end of the receiver after a demodulation. The frequency spectrum should cover $\pm 0.25\,Hz$ of Bragg peaks and $0.75\,Hz$ of Doppler shift caused by the radial component of the moving target. Therefore, maximum frequency (f_{max}) may be set to, for example, $\pm 1.0\,Hz$, or $\pm 2.0\,Hz$. These two yields, for N=512, the frequency resolution of $\Delta f \approx 0.004\,Hz$ and $\Delta f \approx 0.008\,Hz$, respectively. The signal integration time (i.e., recording period) is inversely proportional with the frequency resolution, and is equal to ($T = 1/\Delta f$) 250 s for $\Delta f \approx 0.004\,Hz$. In the figure, the two Bragg peaks around ± 1 and the target around ± 3 normalized frequencies, respectively, are clearly identified. If the CFAR threshold in the detection algorithm is set, let's say, around -15 dB the target will be detected. Note that, there may also be many ghost detections because of the noise and clutter spikes.

4. Conclusions

HFSWR based IMS system is a good solution for maritime traffic surveillance and control. Modeling and numerical simulation is a good alternative for the tests and performance evaluations. Challenging problems are propagation modeling, target reflectivity investigations, synthetic generation of the radar signal environment. HFSWR-based IMS system modeling and simulation necessitates synthetic generation of radar signal environment as realistic as possible. This could only be achieved by good understanding of physical as well as statistical behaviors of radar target, noise, clutter, and interference.

References

[1] L. Sevgi, A. M. Ponsford, H. C. Chan, "An Integrated Maritime Surveillance System Based on Surface Wave HF Radars, Part I – Theoretical Background and Numerical Simulations," *IEEE Antennas and Propagation Magazine*, 43 (4), pp.28-43, Aug. 2001.

[2] A. M. Ponsford, L. Sevgi, H.C. Chan, "An Integrated Maritime Surveillance System Based on Surface Wave HF Radars, Part II – Operational Status and System Performance," *IEEE Antennas and Propagation Magazine*, 43 (5), pp.52-63, Oct. 2001.

[3] A. N. Ince, E. Topuz, E. Panayirci, C. Işık, *Principles of Integrated Maritime Surveillance Systems*, Kluwer Academic, Boston, 2000.

[4] L. Sevgi, *Complex Electromagnetic Problems and Numerical Simulation approaches*, IEEE - John Wiley Press, NJ, May 2003.

[5] CCIR, "Ground wave Propagation Curves for Frequencies Between 10kHz and 30MHz," *CCIR Rec.* 368-6, 1990.

[6] J. R. Wait, "On the Theory of Mixed-path Ground-wave Propagation on a Spherical Earth," *J. Research NBS*, 65D, pp.401-410, 1961

[7] L. Sevgi, "A Numerical Millington Propagation Package for Medium and Short Wave DRM Systems Field Strength Predictions," *IEEE Broadcast Technology Society Newsletter*, 14 (3), pp. 9-11, Fall 2006.

[8] L. Sevgi, "A Mixed-Path Groundwave Field Strength Prediction Virtual Tool for Digital Radio Broadcast Systems in Medium and Short Wave Bands," *IEEE Antennas and Propagation Magazine*, 48 (4), pp.19-27, Aug 2006.

[9] G. Millington, "Ground Wave propagation over an Inhomogeneous Smooth Earth," *Proc. IRE*, Part III, 96 (39), pp.53-64, Jan 1949.

[10] L. Sevgi, F. Akleman, L. B. Felsen, "Ground Wave Propagation Modeling: Problem-matched Analytical Formulations and Direct Numerical Techniques," *IEEE Antennas and Propagation Magazine*, 44 (1), pp.55-75, Feb. 2002.

[11] L. Sevgi, L. B. Felsen, "A new Algorithm for Ground Wave Propagation Problems Based on a Hybrid Ray-Mode Approach," *Int. Journal of Numerical Modeling*, 11 (2), pp.8-103, Mar-Apr 1998.

[12] L. Sevgi, "Modeling and Simulation Strategies for Electromagnetic Wave Propagation in Complex Environments: Groundwave Path Loss Prediction Virtual Tools," *IEEE Transactions on Antennas and Propagation*, 55 (6), pp.1591-1598, Jun 2007.

[13] L. Sevgi, "Novel digital Broadcast/Communication Systems and Groundwave Propagation Prediction Requirements," *EuCAP 2006, The first ESA European Conference on Antennas and Propagation*, Nov 6-10, Nice, 2006.

[14] G. Apaydın, L. Sevgi, "FEM-based surface wave multi-mixed-path propagator and path loss predictions," *IEEE Antennas and Wireless Propagation Letters*, Vol. 8, pp. 1010-1013, Apr. 2009.

[15] G. Apaydın, L. Sevgi, "Numerical Investigations of and Path Loss Predictions for Surface Wave Propagation over Sea Paths Including Hilly Island Transitions," *IEEE Trans. on Antennas and Propagat.* vol.58, No. 4, pp. 1302-1314, June 2009.

[16] L. Sevgi, "Stochastic Modeling of Target Detection and Tracking in Surface Wave High Frequency Radars," *Int. J. of Numerical Modeling*, 11 (3), pp.167-l81, May-Jun 1998.

[17] A. M. Ponsford, S. K. Srivastava, "A Comparison between Measured and Modeled Radar Cross Section from a Ground wave Radar," *Proc. of IEE 5th Int. Conf. on HF Systems and Techniques,* IEE339, pp.61-65, Edinburgh, 1991.

[18] S. K. Srivastava, A. M. Ponsford, "Long Range Detection of Icebergs using Ground wave Radar," *Proc. of Int. Offshore and Polar Eng. Conf.,* 2, pp.471-476, Edinburgh, 1991.

[19] E. D. R. Shearman, "Propagation and Scattering in MF/HF Ground wave Radar," *IEE Proc. F*, 130, pp. 579-590, 1983.

[20] L. Sevgi, "HF Wire Antenna Array Design via FDTD and MoM Techniques," *Proc. of EEE Canadian Conference on Electrical and Computer Engineering*, pp.7-12, May 1999, CA.

[21] L. Sevgi, "Target Reflectivity and RCS Interaction in Integrated Maritime Surveillance Systems Based on Surface Wave HF Radar Radars," *IEEE Antennas and Propagation Magazine*, 43 (1), pp. 36-51, Feb. 2001.

[22] L. Sevgi, S. Paker, "FTDT based RCS Calculations and Antenna Simulations," *AEU, International J. of Electronics and Communication*, 52 (2), pp.65-75, Mar 1998.

[23] CCIR Recommendations, "Characteristics and Applications of Atmospheric Radio Noise Data," *CCIR Rec.* 322-3, 1988.

[24] L. Sevgi, A. M. Ponsford, "Propagation and Interference Characteristics of Surface Wave HF Radars," *URSI, XXVIth General Assembly*, Aug.13-21, 1999, CA.

[25] C. Işık and L. Sevgi, "Atmospheric noise and spectrum occupancy measurements," *Technical Report, UZUN UFUK Project*, Jul-Aug 1996.

[26] D. Barrick, "First Order Theory and Analysis of MF/HF/VHF Scatter from the Sea," *IEEE Trans. Antennas and Propagat.*, AP-20, pp.2-10, 1972.

[27] K. Hasselman, "Determination of Ocean Wave Spectra from Doppler Radio Return from the Sea Surface," *Nature Phys. Sci.*, 229, pp. 16-17, 1971.

[28] R. Howell, J. Walsh, "Measurement of Ocean Wave Spectra using Narrow Beam HF Radar," *Proc. of 12th Can. Symp. on Remote Sensing, IGARSS'89*, Vancouver, BC, 5, pp.2969-2972. 1989.

[29] B.J. Lipa, D.F. Barrick, "Extraction of Sea State from HF Radar Sea Echo," *Radio Sci.,* 21, pp. 81-100, 1986.

[30] L. R. Wyatt, "The Measurement of the Ocean Wave Directional Spectrum from HF Radar Doppler Spectra," *Radio Sci.,* 21, pp 473-485, 1986.

[31] F. Gott, N. F. Wong, S. Dutta, "Occupancy Measurements Across the Entire HF Spectrum," *AGARD Conf. Publ.* 332, Paris 1982.

[32] Ç. Uluışık, G. Çakır, M. Çakır, L. Sevgi, "Radar Cross section (RCS) Modeling and Simulation: Part I – Definitions, Strategies, and Canonical Examples," *IEEE Antennas and Propagation Magazine*, 50 (1), pp.115-126, Feb 2008.

[33] G. Çakır, M. Çakır, L. Sevgi, "Radar Cross section (RCS) Modeling and Simulation: Part II – A Novel FDTD-Based RCS Prediction Virtual Tool," *IEEE Antennas and Propagation Magazine*, 50 (2), pp.81-94, Apr 2008.

[34] L. Sevgi, "Synthetic Radar Signal Environment: Computer Generation of Signal, Noise, and Clutter," *IEEE Antennas and Propagation Magazine*, 49 (5), pp.192-198, Oct 2007.